

Estimation of shear strength of very coarse mine waste

S Linero-Molina *SRK Consulting, Australia*

LF Contreras *SRK Consulting, Australia*

J Dixon *Fortescue Metals Group, Australia*

Abstract

Evaluating the shear strength of mine waste rock containing particles of metric scale is challenging because commercial laboratory testing devices can only accommodate samples composed of particles a few centimetres in size. The shear strength empirical model of Barton & Kjærnsli (1981) is therefore frequently used to assess the non-linear shear strength of very coarse granular material for stability assessment of very high mine waste dumps. In this article, we discuss practical methods for collecting the information required as input to the model, and we also illustrate the implementation of deterministic and probabilistic approaches for estimating the shear strength of several waste materials from a banded iron formation located in the Pilbara region of Western Australia.

Keywords: *shear strength, very coarse granular material, mine waste dumps*

1 Introduction

Evaluating the shear strength of mine waste rock containing particles of metric scale is challenging because commercial laboratory testing devices can only accommodate samples composed of particles a few centimetres in size. To overcome testing limitations, the shear strength is frequently estimated using the shear strength empirical model of Barton & Kjærnsli (1981) (B–K criterion), which considers the nonlinearity of the shear strength envelope, characterising the behaviour of very coarse granular materials submitted to very high loads (Leps 1970; Ovalle et al. 2020).

In the B–K criterion, a stress-dependent structural component of the shear strength is parametrised with the equivalent roughness (R) and equivalent strength (S). The structural component is added to the basic friction angle (φ_b) of the parental rock to determine the shear strength of the waste rock material. Barton modelled this criterion using R and S as equivalent to his joint roughness coefficient and joint wall compression strength in his shear strength criterion for rock joints (Barton 1973) (i.e. asperity and particle contact in common). In this paper, different methods are discussed to gather the information required for the practical implementation of the B–K model, and deterministic and probabilistic approaches are presented for the shear strength determination of coarse waste for waste dump design. The approaches are illustrated using the information gathered for a project where the waste rock materials originated during mining activities from a banded iron formation in the Pilbara region of Western Australia.

2 Strength model for coarse granular materials

The B–K empirical non-linear model is represented by Equation 1. The model is intended to be utilised for characterising coarse materials like rockfill and blasted rocks, which typically undergo crushing under the imposed loads and therefore exhibit a non-linear shear strength envelope. In the B–K model, the effective friction angle of the waste rock is estimated by adding to the basic angle of friction (φ_b) a structural component of strength (which is stress-dependent), determined by the degree of roundness of the particles and the porosity of the arrangement of particles. According to the expression, the friction angle is at least equal to the basic friction angle and varies in a magnitude R for a 10-fold increase of S/σ_n .

$$\Phi' = \varphi_b + R \text{Log}_{10} (S/\sigma_n) \quad (1)$$

where:

- φ' = effective friction angle.
- φ_b = basic friction angle of the rock.
- R = equivalent roughness of waste particles.
- S = size-dependent equivalent strength of waste particles.

The parameter R is a function of particles roundness and porosity (n) of the arrangement of particles. It is determined based on the chart proposed by Barton-Kjærnsli, presented in Figure 1a. R may vary between 0 and 15 for loose arrangements of rounded, very smooth particles to dense arrangements of very angular and rough particles, respectively. The parameter S is a function of the unconfined compressive strength (UCS) of the rock and its characteristic particle size, adopted here as the median diameter by weight (D_{50}). It is determined based on the chart presented in Figure 1b. When large-scale laboratory results are available, R and S can be defined using Bayesian statistics, as described by Linero et al. (2022), for customisation of those parameters to the material being analysed.

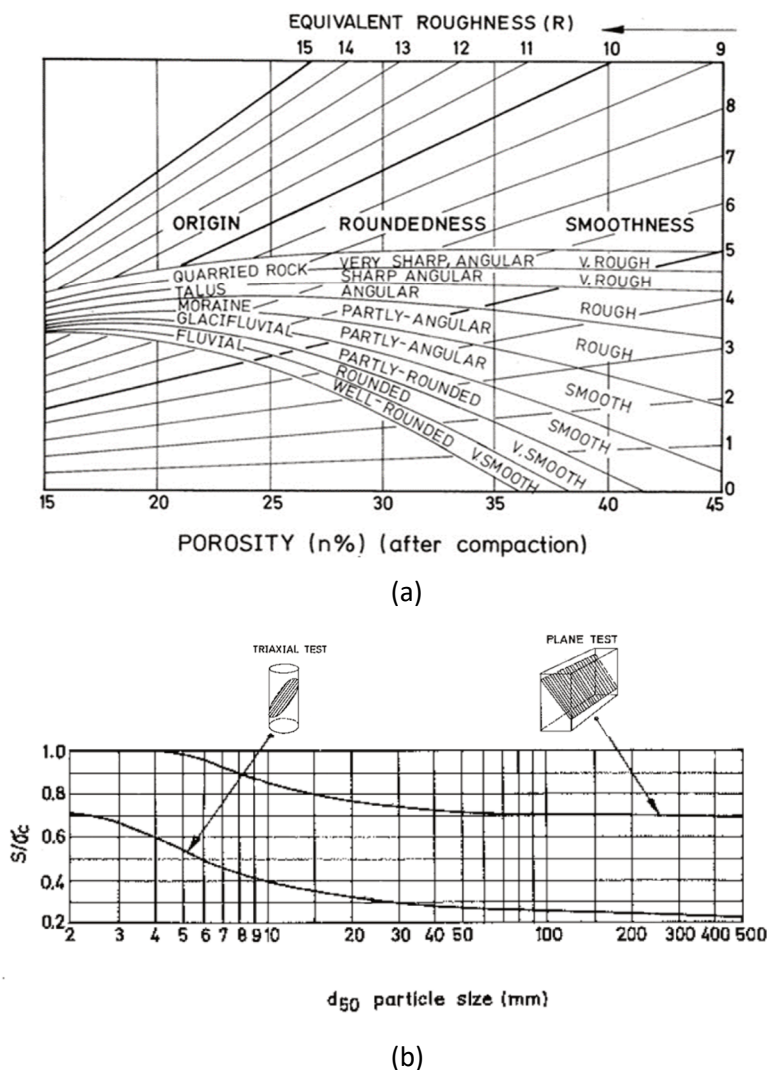


Figure 1 Charts proposed by Barton-Kjærnsli (1981) (a) for estimation of equivalent roughness and (b) for estimation of equivalent strength

3 Strength model parameters

The parameters discussed below are evaluated to be fed directly or indirectly into the model.

3.1 Basic friction angle

The basic friction angle φ_b can be estimated in tilting tests using dry, sawn surfaces of the parental rock (Barton & Kjærnsli 1981). In the mining context, it is more often obtained from direct shear tests conducted on saw-cut samples selected from drill cores. In this case, φ_b is calculated as the inverse of the tangent of shear stress divided by the normal stress for each determination (zero cohesion). This information is usually readily available in the geotechnical drillhole database, as it is also used for rock mass characterisation for pit design purposes. Figure 2 illustrates typical results of this parameter. The availability of data usually varies across the different units, so core sampling and supplemental testing may be required.

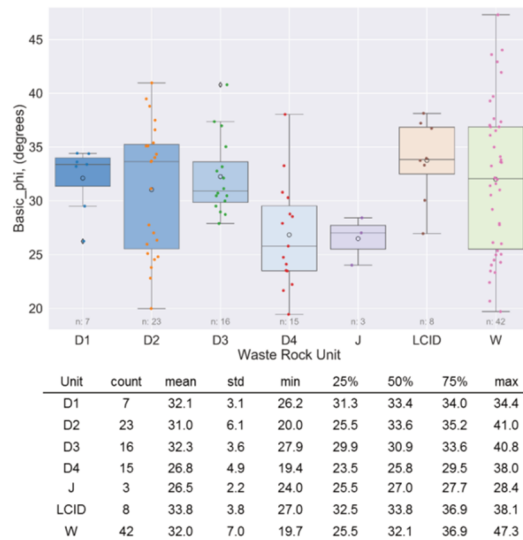


Figure 2 Characteristics of the basic friction angle of the waste rock units

3.2 Unconfined compressive strength

The UCS can be obtained by testing selected core samples, although this information is also usually available in the geotechnical drillhole database and frequently far more abundant than the information on φ_b . Point load testing (PLT) data and Schmidt hammer rebound determinations are also usually considered, provided that a correlation between UCS and PLT or Schmidt hammer values can be obtained by analysing paired data. The information collected for the waste rock units evaluated is summarised in Figure 3.

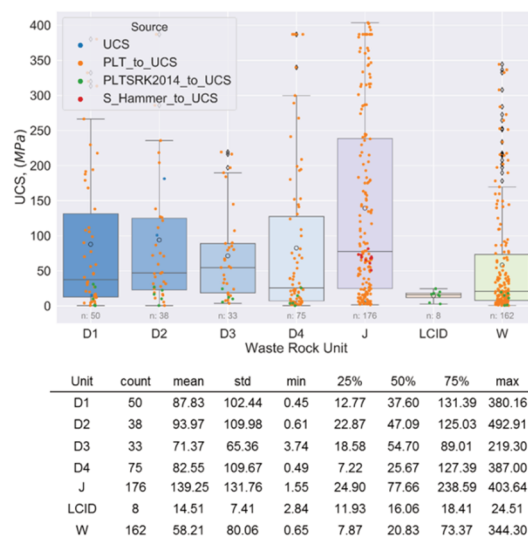


Figure 3 Characteristics of the unconfined compressive strength of the waste rock units

3.3 Porosity of the dumped waste

The unit weight of the solids in the rock fragments (γ_s) is required for estimating the porosity of the dumped waste rock. It can be evaluated based on the dry density of the rock fragments and rock porosity. This information is typically available in the geotechnical drillhole database, as this parameter is determined in conjunction with triaxial testing, and when evaluating elastic properties. Figure 4a shows the γ_s characteristics of the units evaluated.

The dry density (γ_d) of the dumped waste material at large-scale can be estimated by reconciliation of the haul-weight and volume in waste dumps, large-scale dumped piles, or truck hoppers. In the first case, topography from LiDAR surveys from pre-mining and at-the-time-of-the evaluation is compared. For the case of piles, at least 20 t of material are required, as illustrated in Figure 4b for unit D4. When based on truck hoppers, the measurements are made with automatised truckload scanners. The latter method was used to collect the data of the unclassified material presented in the box plot of Figure 4b.

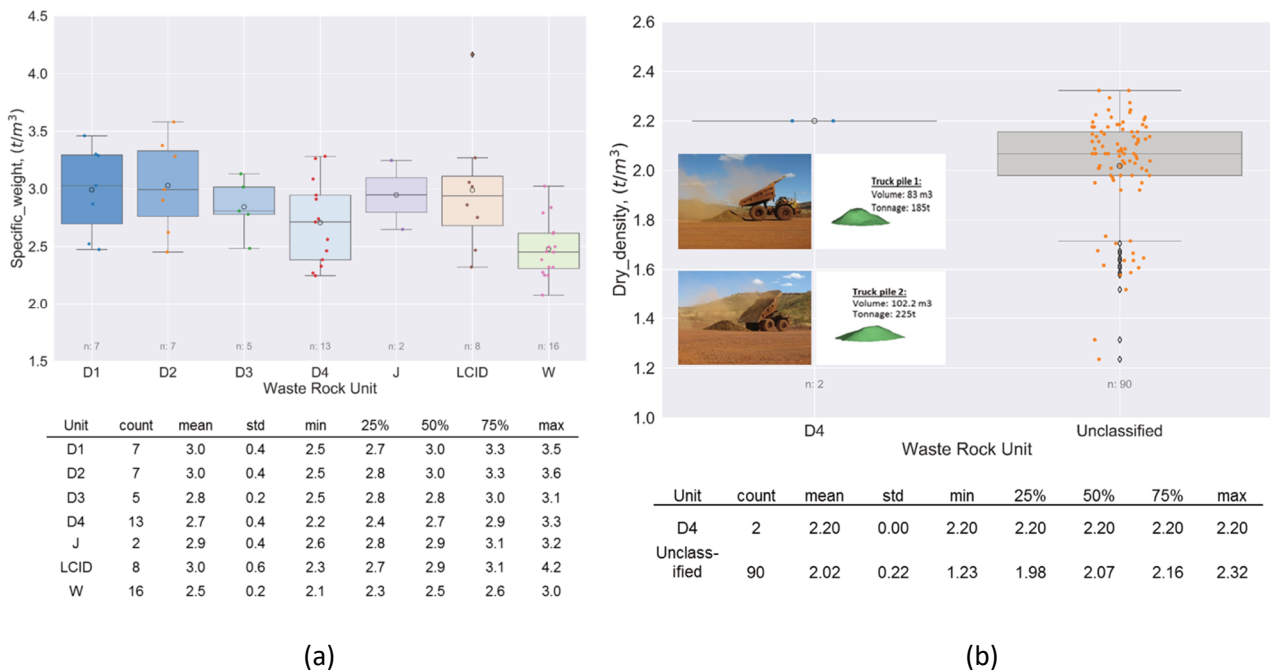


Figure 4 (a) Characteristics of the population of specific weight data by waste rock unit; (b) Distribution of data on dry density of dumped waste

The porosity (n) is calculated based on the dry density (γ_d) of the dumped waste and the specific weight of the particles (γ_s) according to Equation 2:

$$n = 1 - \gamma_d / \gamma_s \tag{2}$$

A waste porosity varying with a uniform distribution between 20 and 35% was adopted to characterise the waste rock units, based on the results of the evaluation.

3.4 Characteristic particle diameter D_{50}

The method for evaluating particle size distribution depends on the maximum particle size, as shown in Table 1. Samples are normally taken from the pit face after blasting, to prevent biased results as a consequence of the inevitable segregation of rehandled material. At feasibility level of design, information on blasting fragmentation is also useful to gain an idea of the expected particle size distribution (PSD). Other indirect techniques are also used, although a calibration/verification of the results is usually necessary. This refers to processing of photos using automatised image recognition algorithms. The PSDs shown in Figure 5

for the waste units evaluated were processed using Split-Net images (www.spliteng.com/products/split-net-service).

Table 1 Particle size distribution evaluation

| Maximum particle size | Sample size | Method |
|-----------------------|--------------------------|---|
| 500 to 2,000 mm | Up to 20 t | Spread on a clean flat area a known weight of material. Equipment aided, set aside count and measure fragments 500 mm and larger to estimate its weight. Count and weigh onsite clasts >250mm. Quarter the smaller fraction and send to the lab for total weight and particle size distribution (PSD) determination. Compose the PSD. |
| Less than 250 mm | Up to one m ³ | Set the sample in 1 m ³ bulk bag for large-scale lab determination of the PSD. |

Note: the sample size should be enough to contain some of the larger fragments so that the resulting PSD represents the material.

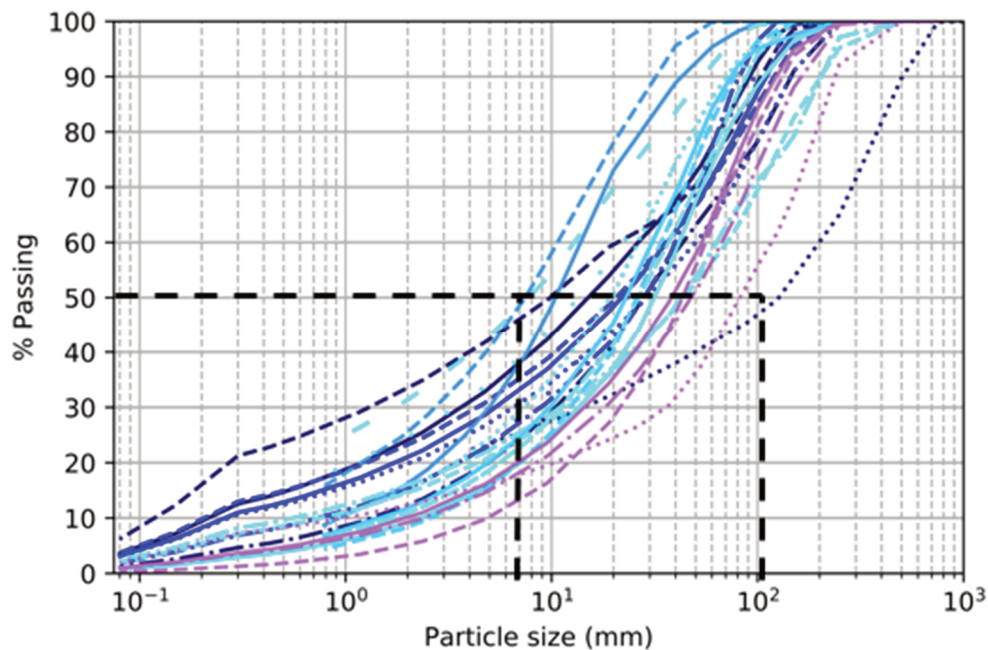


Figure 5 Particle size distribution of waste rock units and identification of D_{50}

4 Shear strength for design with the B–K model

There are two alternative procedures to determine the shear strength for design. The deterministic approach is based on using conservative estimates of the input parameters derived from testing while the probabilistic approach uses full probability distributions of these parameters to account for their uncertainty. A description of these methodologies is presented in the following section.

4.1 Deterministic approach

The conceptual basis of the deterministic approach for the estimation of the strength parameters for design is presented in Figure 6. The base case value corresponds to φ calculated with the B–K equation using the mean values of the component parameters in the model, i.e. φ_b , UCS , D_{50} and n . The D_{50} and n values correspond to the middle point of the ranges considered appropriate for the analysed wastes, based on judgement. These ranges are 6–100 mm for D_{50} and 20–35% for n . The mean values of φ_b and UCS are supported by the data described previously. The example illustrated in Figure 6 corresponds to the unit D3

for a σ_n of 1.5 MPa. The base case φ is 39.8° and the design value is 33.4°, which is based on using the 25th percentile values of φ_b and UCS instead of their mean values. The design value is 6.4° lower in this particular situation and is intended to account for the uncertainty in the estimation of φ_b and UCS from laboratory testing.

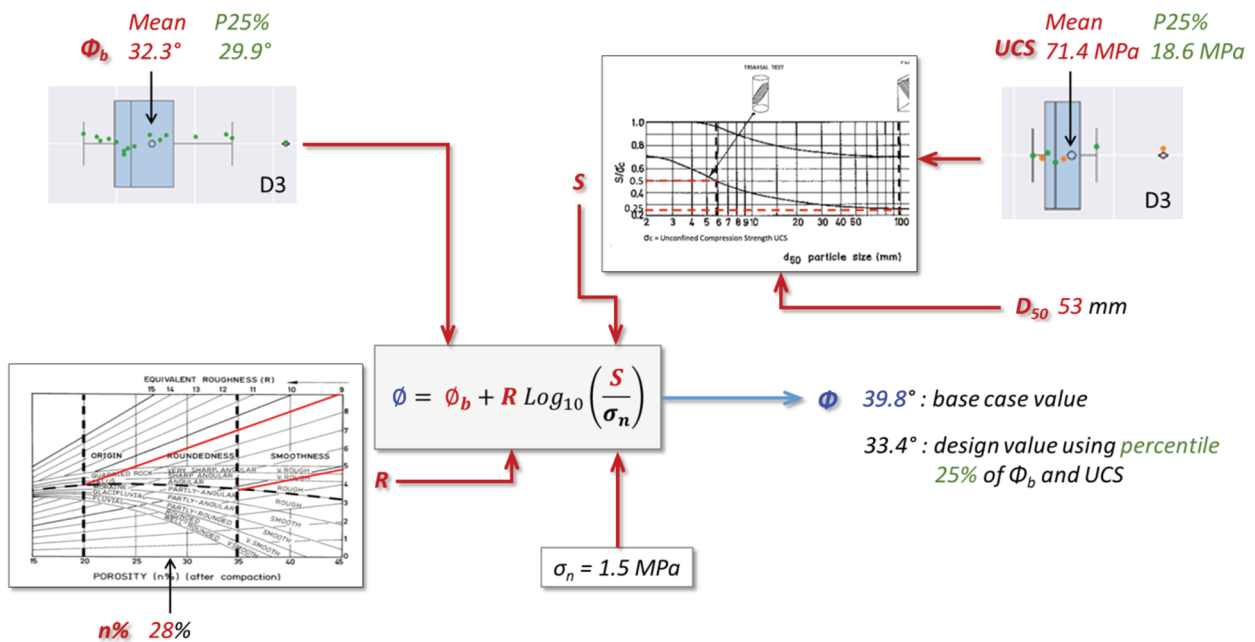


Figure 6 Conceptual description of the deterministic analysis of strength

The results of the deterministic evaluation of the strength of rock wastes are summarised in Figure 7 and Table 2. These results indicate a considerable reduction of φ particularly for the D2, D4 and W units, with differences in excess of 9° in relation to the base case values. In general, these differences are relatively large for all the units except LCID, because the UCS contains a proportion of high values that push the means far apart from the 25th percentile values. This method of calculation does not account for the structure of the dataset, which is an aspect that is taken into account with the probabilistic analysis.

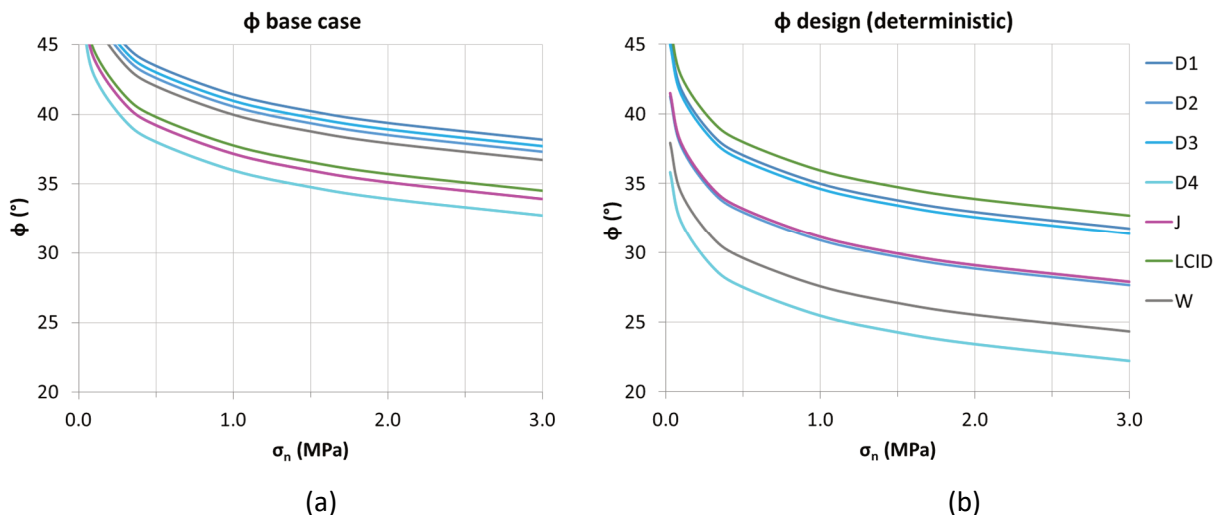


Figure 7 Shear strength of rock wastes from deterministic analysis. (a) Base case values; (b) Design values calculated using P25 values for Φ_b and UCS

Table 2 Results of the deterministic analysis of waste rock strength

| σ_n (MPa) | D1 | D2 | D3 | D4 | J | LCID | W |
|-------------------------------|------|------|------|------|------|------|------|
| ϕ base case | | | | | | | |
| 0.03 | 51.8 | 50.9 | 51.3 | 46.3 | 47.5 | 48.1 | 50.3 |
| 0.1 | 48.2 | 47.4 | 47.8 | 42.8 | 44.0 | 44.6 | 46.8 |
| 0.3 | 45.0 | 44.1 | 44.5 | 39.5 | 40.7 | 41.3 | 43.5 |
| 0.5 | 43.5 | 42.6 | 43.0 | 38.0 | 39.2 | 39.8 | 42.0 |
| 1.0 | 41.4 | 40.6 | 41.0 | 36.0 | 37.2 | 37.8 | 40.0 |
| 1.5 | 40.2 | 39.4 | 39.8 | 34.8 | 36.0 | 36.6 | 38.8 |
| 2.0 | 39.4 | 38.5 | 38.9 | 33.9 | 35.1 | 35.7 | 37.9 |
| 3.0 | 38.2 | 37.3 | 37.7 | 32.7 | 33.9 | 34.5 | 36.7 |
| ϕ design (deterministic) | | | | | | | |
| 0.03 | 45.3 | 41.2 | 45.0 | 35.8 | 41.5 | 46.3 | 37.9 |
| 0.1 | 41.8 | 37.7 | 41.4 | 32.3 | 37.9 | 42.7 | 34.4 |
| 0.3 | 38.5 | 34.4 | 38.2 | 29.0 | 34.7 | 39.5 | 31.1 |
| 0.5 | 37.0 | 32.9 | 36.7 | 27.5 | 33.2 | 38.0 | 29.6 |
| 1.0 | 35.0 | 30.9 | 34.6 | 25.5 | 31.1 | 35.9 | 27.6 |
| 1.5 | 33.8 | 29.7 | 33.4 | 24.3 | 29.9 | 34.7 | 26.4 |
| 2.0 | 32.9 | 28.8 | 32.6 | 23.4 | 29.1 | 33.9 | 25.5 |
| 3.0 | 31.7 | 27.6 | 31.4 | 22.2 | 27.9 | 32.7 | 24.3 |
| Difference | | | | | | | |
| 0.03 | 6.5 | 9.7 | 6.4 | 10.5 | 6.1 | 1.8 | 12.4 |
| 0.1 | 6.5 | 9.7 | 6.4 | 10.5 | 6.1 | 1.8 | 12.4 |
| 0.3 | 6.5 | 9.7 | 6.4 | 10.5 | 6.1 | 1.8 | 12.4 |
| 0.5 | 6.5 | 9.7 | 6.4 | 10.5 | 6.1 | 1.8 | 12.4 |
| 1.0 | 6.5 | 9.7 | 6.4 | 10.5 | 6.1 | 1.8 | 12.4 |
| 1.5 | 6.5 | 9.7 | 6.4 | 10.5 | 6.1 | 1.8 | 12.4 |
| 2.0 | 6.5 | 9.7 | 6.4 | 10.5 | 6.1 | 1.8 | 12.4 |
| 3.0 | 6.5 | 9.7 | 6.4 | 10.5 | 6.1 | 1.8 | 12.4 |
| Legend | | | | | | | |
| <3 | | 3–6 | | 6–9 | | >9 | |

4.2 Probabilistic approach

The probabilistic approach is based on a Monte Carlo (MC) analysis to simulate the variability of the component parameters in the B–K strength model represented with the expression included in Equation 1. The conceptual explanation of the probabilistic analysis is sketched in Figure 8 using information from the

analysis of unit D3 for effective normal stress (σ_n) of 1.5 MPa. The diagram shows the distinction between the base case value, the design value from the deterministic calculation and the value from the probabilistic analysis with a 75% level of confidence.

The basic friction angle (ϕ_b) and the UCS were represented by probability distributions derived from the available test results, as shown in Tables 3 and 4. In this case, all data points were considered without the screening of the so-called outliers, since this process is subjective and it was not deemed necessary with this approach. The probability distributions were intended to account for the uncertainty of the parameters and were based on the observed variability of the data as well as judgement to include the uncertainty due to insufficiency of data. The characteristics of the distributions of ϕ_b were defined using a fitting procedure when the number of data points was 15 or more and normal distributions were assumed in the other cases with the mean and standard deviation of the available data points. The number of UCS data points was sufficient to define fitted distributions, however, the results of the fitting analysis seemed unrealistic, and it was judged that the fitted distributions might not represent this property adequately. Therefore, the UCS distributions were assumed to be lognormal with the mean and standard deviation of the respective datasets.

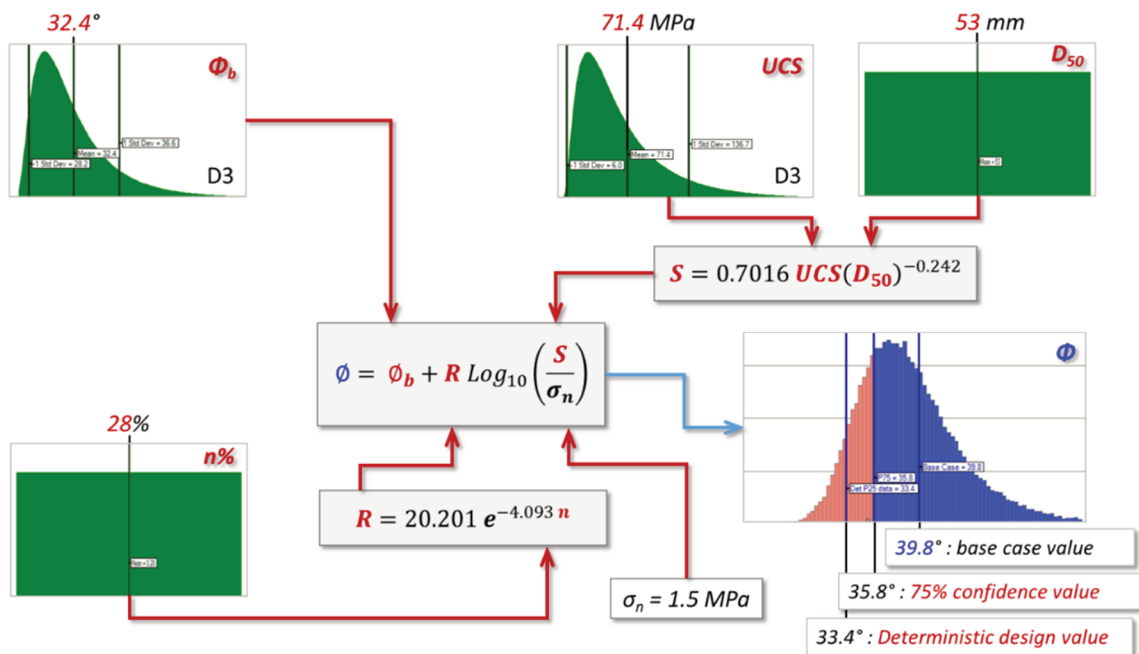


Figure 8 Conceptual description of the probabilistic analysis of strength

The variability of Barton’s equivalent roughness (R) is based on assuming a uniform distribution for the porosity (n) between 20% and 35% and considering the ‘talus-angular-rough’ condition in Barton’s chart (Figure 1a). The expression that captures the variability of R for these conditions is:

$$R = 20.201 e^{-4.093 n} \tag{3}$$

The variability of Barton’s equivalent strength (S) considers the variability of UCS defined for the respective rock type and assumes a uniform variability of D_{50} between 6 mm and 100 mm for the triaxial test curve in Barton’s chart (Figure 1b). The equation reflecting the variability of S for these conditions is:

$$S = 0.702 UCS (D_{50})^{-0.242} \tag{4}$$

Table 3 Distributions representing the variability of base friction angle

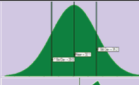
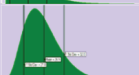
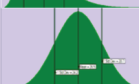
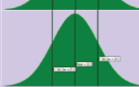
| Unit | No. tests | Data | | Distribution | | | Mode | Min | Max | Picture | Comment |
|------|-----------|------|--------------------|--------------|------|--------------------|------|------|------|---|---------|
| | | Mean | Standard deviation | Type | Mean | Standard deviation | | | | | |
| D1 | 7 | 32.1 | 3.1 | Normal | 32.1 | 3.1 | | | |  | Assumed |
| D2 | 23 | 31.0 | 6.1 | Triangular | | | 35.4 | 15.6 | 43.6 |  | Fitted |
| D3 | 16 | 32.3 | 3.6 | Lognormal | 32.4 | 4.2 | | | |  | Fitted |
| D4 | 15 | 26.8 | 4.9 | Lognormal | 26.9 | 5.1 | | | |  | Fitted |
| J | 3 | 26.5 | 2.2 | Normal | 26.5 | 2.2 | | | |  | Assumed |
| LCID | 8 | 33.8 | 3.8 | Normal | 33.8 | 3.8 | | | |  | Assumed |
| W | 42 | 31.9 | 7.0 | Normal | 32.0 | 7.0 | | | |  | Fitted |

Table 4 Distributions representing the variability of the unconfined compressive strength

| Unit | No. tests | Data | | Distribution | | | Picture | Comment |
|------|-----------|-------|--------------------|--------------|-------|--------------------|---|---------|
| | | Mean | Standard deviation | Type | Mean | Standard deviation | | |
| D1 | 50 | 87.8 | 102.4 | Lognormal | 87.8 | 102.4 |  | Assumed |
| D2 | 38 | 94.0 | 110.0 | Lognormal | 94.0 | 110.0 |  | Assumed |
| D3 | 33 | 71.4 | 65.4 | Lognormal | 71.4 | 65.4 |  | Assumed |
| D4 | 75 | 82.5 | 109.7 | Lognormal | 82.5 | 109.7 |  | Assumed |
| J | 176 | 139.3 | 131.8 | Lognormal | 139.3 | 131.8 |  | Assumed |
| LCID | 8 | 14.5 | 7.4 | Lognormal | 14.5 | 7.4 |  | Assumed |
| W | 162 | 58.2 | 80.1 | Lognormal | 58.2 | 80.1 |  | Assumed |

The MC analysis is carried out with 100,000 trials, assuming that the four input variables are independent. The result of the analysis provides the information to construct the output probability distributions of friction angle (φ) for a range of effective normal stresses (σ_n) between 0.5 MPa and 3.0 MPa. This calculation is carried out for each waste rock unit considering the respective input parameters. Figure 9 presents the results of the probabilistic analysis.

The graph on the left (Figure 9a) corresponds to the base case situation using the mean values of the datasets and is the same result shown for the deterministic analysis. The graph on the right (Figure 9b) shows the 75% confidence strength estimation, which corresponds to the 25th percentile of the distributions of φ resulting from the MC analysis.

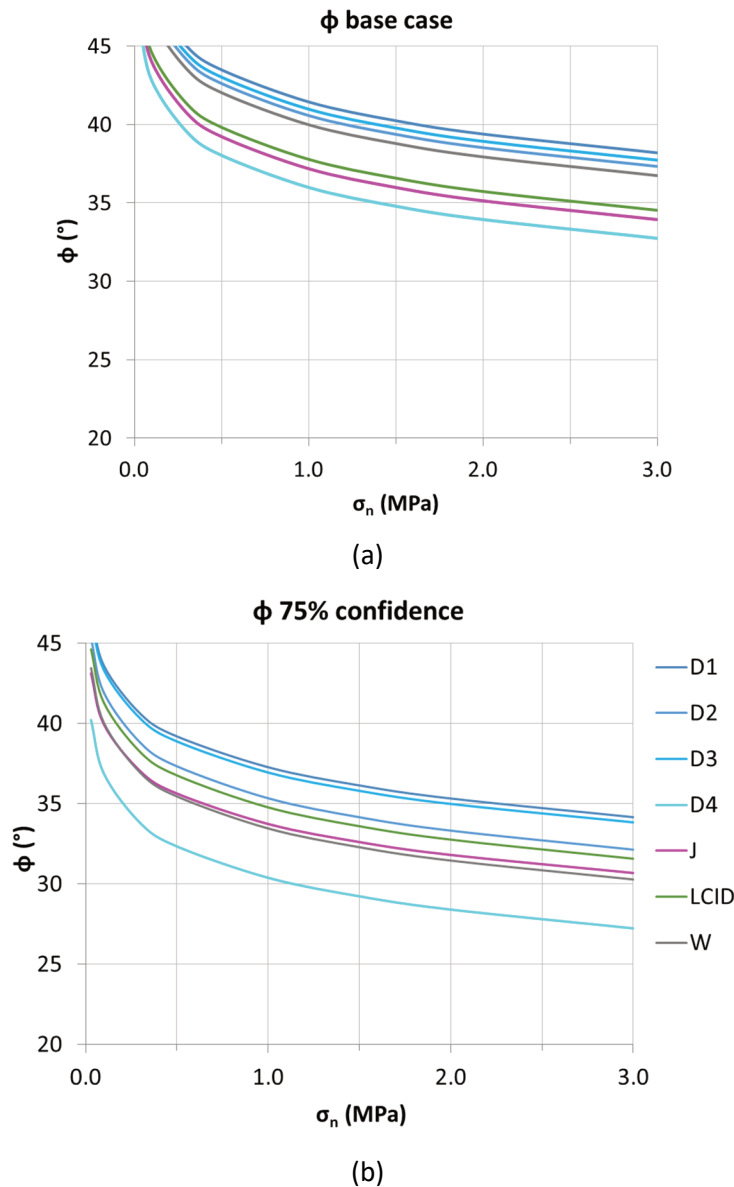


Figure 9 Shear strength of rock wastes from probabilistic analysis. (a) Base case values; (b) 75% confidence values proposed for design

The results of the probabilistic analysis are presented in Table 5 to facilitate their inspection. The difference between the base case and the 75% confidence values is a reflection of the uncertainty of the estimation represented by the spread of the output distribution. This difference varies from 3.0° for the unit LCID up to 6.9° for the unit W. The unit W has good UCS data support with 162 values but still has the largest differences, which suggests that it is not only the number of data points but the quality of the data that matters in reducing the uncertainty of the estimation. For instance, it appears that some of the datasets combine information from various subunits characterised by different degrees of weathering, causing a widespread of the input distributions.

The comparison between the results from the deterministic calculation (Table 2) and the probabilistic analysis (Table 5) shows that in general, the differences between the base case values of ϕ and the values accounting for uncertainty are smaller for the probabilistic calculation. This is because the probabilistic analysis takes into account the structure of the datasets and considers the propagation of the uncertainty of the parameters through the calculation process.

Table 5 Results of the probabilistic analysis of waste rock strength

| σ_n (MPa) | D1 | D2 | D3 | D4 | J | LCID | W |
|-----------------------|------|------|------|------|------|------|------|
| ϕ base case | | | | | | | |
| 0.03 | 51.8 | 50.9 | 51.3 | 46.3 | 47.5 | 48.1 | 50.3 |
| 0.1 | 48.2 | 47.4 | 47.8 | 42.8 | 44.0 | 44.6 | 46.8 |
| 0.3 | 45.0 | 44.1 | 44.5 | 39.5 | 40.7 | 41.3 | 43.5 |
| 0.5 | 43.5 | 42.6 | 43.0 | 38.0 | 39.2 | 39.8 | 42.0 |
| 1.0 | 41.4 | 40.6 | 41.0 | 36.0 | 37.2 | 37.8 | 40.0 |
| 1.5 | 40.2 | 39.4 | 39.8 | 34.8 | 36.0 | 36.6 | 38.8 |
| 2.0 | 39.4 | 38.5 | 38.9 | 33.9 | 35.1 | 35.7 | 37.9 |
| 3.0 | 38.2 | 37.3 | 37.7 | 32.7 | 33.9 | 34.5 | 36.7 |
| ϕ 75% confidence | | | | | | | |
| 0.03 | 46.9 | 45.3 | 46.6 | 40.2 | 43.1 | 44.6 | 43.5 |
| 0.1 | 43.6 | 41.9 | 43.3 | 36.9 | 40.0 | 41.3 | 40.0 |
| 0.3 | 40.6 | 38.8 | 40.3 | 33.8 | 37.0 | 38.2 | 36.9 |
| 0.5 | 39.2 | 37.3 | 38.9 | 32.3 | 35.6 | 36.8 | 35.5 |
| 1.0 | 37.3 | 35.3 | 36.9 | 30.4 | 33.7 | 34.8 | 33.5 |
| 1.5 | 36.1 | 34.2 | 35.8 | 29.2 | 32.6 | 33.6 | 32.3 |
| 2.0 | 35.3 | 33.3 | 35.0 | 28.4 | 31.8 | 32.8 | 31.5 |
| 3.0 | 34.2 | 32.1 | 33.8 | 27.2 | 30.7 | 31.6 | 30.3 |
| Difference | | | | | | | |
| 0.03 | 4.9 | 5.6 | 4.7 | 6.1 | 4.4 | 3.5 | 6.9 |
| 0.1 | 4.6 | 5.4 | 4.4 | 5.9 | 4.0 | 3.3 | 6.7 |
| 0.3 | 4.4 | 5.3 | 4.2 | 5.7 | 3.7 | 3.1 | 6.6 |
| 0.5 | 4.3 | 5.3 | 4.1 | 5.7 | 3.6 | 3.1 | 6.6 |
| 1.0 | 4.2 | 5.2 | 4.0 | 5.6 | 3.4 | 3.0 | 6.5 |
| 1.5 | 4.1 | 5.2 | 4.0 | 5.6 | 3.4 | 3.0 | 6.5 |
| 2.0 | 4.1 | 5.2 | 3.9 | 5.5 | 3.3 | 3.0 | 6.5 |
| 3.0 | 4.0 | 5.2 | 3.9 | 5.5 | 3.2 | 3.0 | 6.5 |
| Legend | | | | | | | |
| <3 | | 3–6 | | 6–9 | | >9 | |

A by-product of the probabilistic analysis is the evaluation of the sensitivity of ϕ' to the variability of the uncertain parameters. The results of the sensitivity analysis are presented in tornado graphs that show the relative effect of the input parameters on the calculated ϕ' . Figure 10 presents the results of the MC analysis for unit D3 with $\sigma_n = 1.5$ MPa; the probability distribution is shown in Figure 10a and the respective tornado graph is included in Figure 10b. This result indicates that the variability of the basic friction angle contributes

59% to the variance of φ' , followed by the UCS with 31%. The negative values for n and D_{50} correspond to a convention indicating that these parameters have an inverse correlation with φ ; hence, the sum of the absolute values of the four contributions adds to 100%.

The selection of the appropriate φ' for design should take into consideration the typical spatial variability characteristics of the waste. The spatial variability of a property is normally represented by random fields that are defined by the mean, standard deviation, and the correlation length of the property. The spatial correlation length may be interpreted as the distance beyond which the correlation is weak, and the values are almost independent. If the waste conditions correspond to a small correlation length relative to the length of potential slip surfaces, then the equivalent strength of the slip surface in a slope stability analysis may be close to the mean strength of the waste. However, if the correlation length is comparable to the length of the potential slip surface or if the material is segregated in such a way that the slip surface might not be represented by a mix of different strength values, then the equivalent strength of the slip surface in a slope stability analysis could be a low value far from the mean.

Renani et al. (2019) suggest the use of an equivalent strength obtained by reducing the mean strength by one-third of its standard deviation to account for the spatial variability of rock properties in slope stability analysis. This criterion has been represented for comparison purposes in the probability distribution of φ for unit D3 and $\sigma_n = 1.5$ MPa in Figure 10. However, this criterion is meant to be used to adjust the UCS in rock slopes with situations of small correlation length. In conclusion, it is important to understand the spatial variability conditions of the rock wastes and their relationship with the expected lengths of the potential slip surfaces, as well as the extent of the domains represented by the probability distributions of the properties, to support the judgement in the selection of the adequate criterion for design.

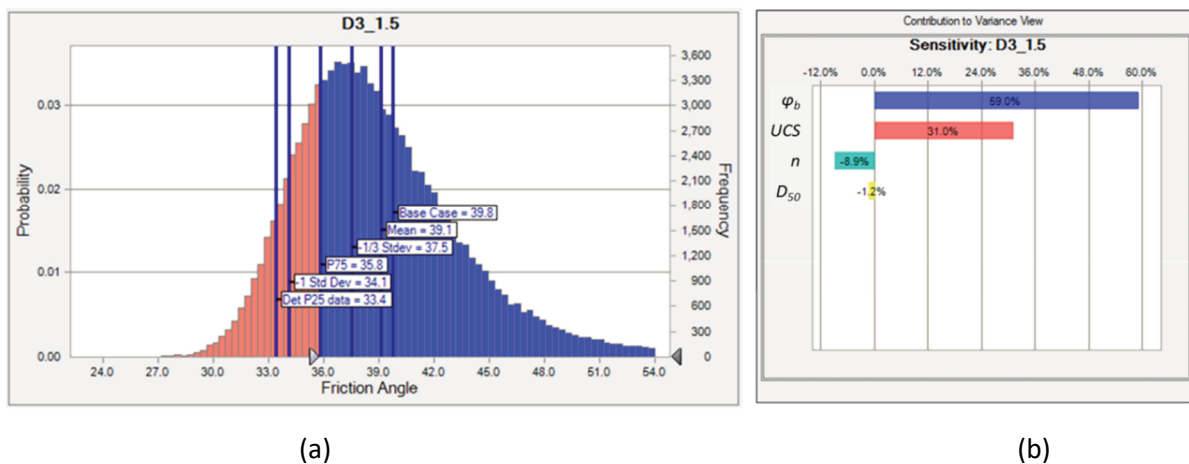


Figure 10 Results of the Monte Carlo analysis for unit D3 and $\sigma_n = 1.5$ MPa. (a) Comparison of different criteria for the selection of the design value of φ' ; (b) Tornado graph with the sensitivity analysis of φ'

5 Use of the results of the strength characterisation

The strength characterisation results consist of conservative φ values for the ranges of σ_n evaluated (Figures 7 and 9) or alternatively, full probability distributions of φ for the respective σ_n values (i.e. Figure 10). The first result is intended to be used for the deterministic analysis of stability of the waste dumps, the second could be used to derive the appropriate conservative values based on a selected confidence level considered adequate for specific situations. These conservative estimates of strength are meant to be used as best estimates of φ in deterministic analysis of stability.

The difficulty for the deterministic slope stability analysis is the selection of the appropriate strength estimate that is consistent with the spatial variability characteristics of the waste dump. Figure 11 shows a conceptual representation of how two different spatial distributions of φ could influence the equivalent strength of a potential slip surface in the slope. The spatial variability in Figure 11 is represented by random fields, which

are defined by the mean, standard deviation and length of correlation of φ in this example. The length of correlation in the slope to the left in Figure 11a is small compared to the length of the slip surface and the equivalent strength for the failure surface is probably closer to the mean of the random field. In contrast, when the length of correlation is comparable to the length of the slip surface as depicted for the slope to the right in Figure 11b, the equivalent strength of the failure surface is probably far from the mean of the random field and likely determined by the low strength zones (in blue) of the random field. The mean and standard deviation of φ are defined with the probabilistic analysis described before and reflected in the histogram shown in Figure 10. The determination of the length of correlation requires systematic sampling and testing of the dumps, which would be unfeasible in practice. However, a reasonable estimation of the spatial distribution of the properties could be obtained from detailed photographic mapping of the waste dump faces over a suitable time period to identify patterns of segregation of the material.

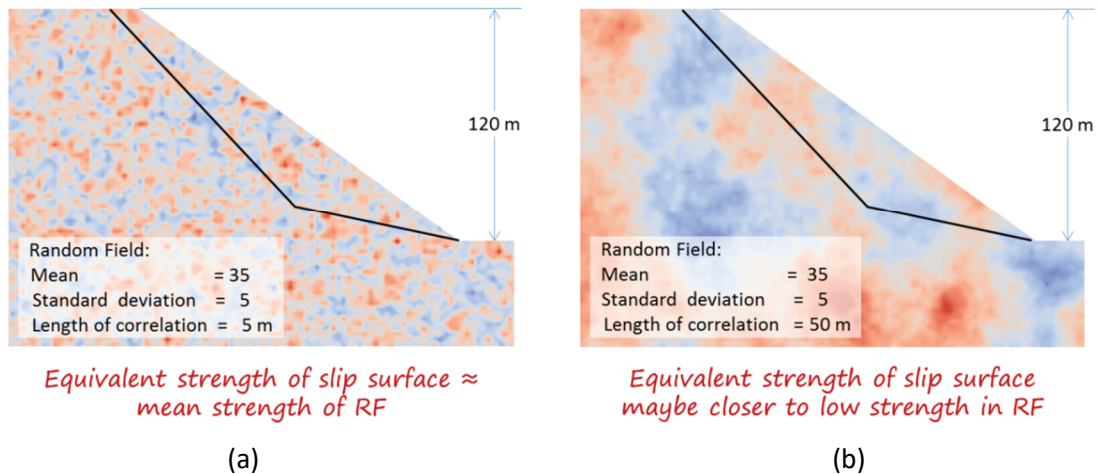


Figure 11 Conceptual illustration of the effect of the spatial variability of the strength on the equivalent strength for stability analysis. (a) Random field of a property with mean 35, standard deviation 5 and length of correlation 5 m; (b) Random field with length of correlation increased to 50 m

Figure 12 shows a more realistic representation of the spatial distribution of the geomechanical properties of the waste dump based on the observed conditions of an excavated cross-section of a waste dump (Hawley & Cuning 2017). This conceptual representation of the spatial variability of the material characteristics would enable the definition of a more realistic slope model for stability analysis, where the various zones could be characterised more precisely and the appropriate design values, perhaps closer to the mean, could be selected.

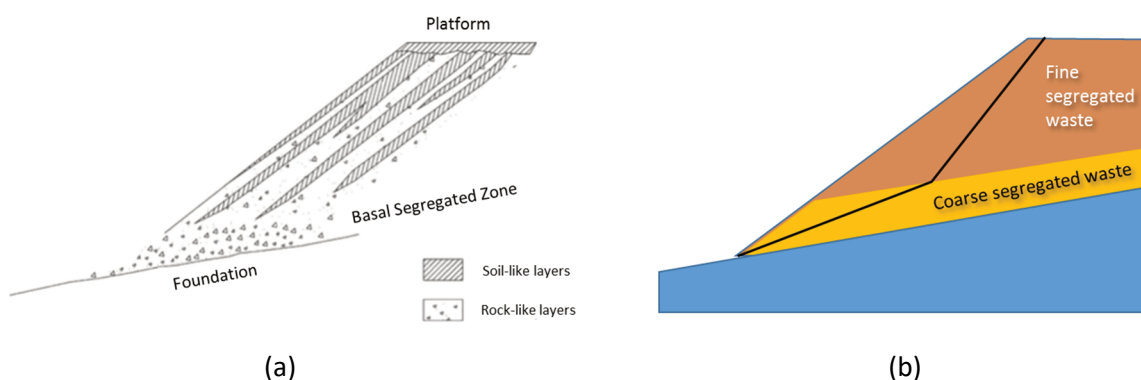


Figure 12 Idealisation of waste dump for a slope stability analysis. Notes: (a) Typical stratigraphy of an end-dumped waste dump. Source: Hungr et al. (2002) in Hawley & Cuning (2017), and (b) Suggested slope model for stability analysis

6 Summary and conclusion

The methodology to characterise the shear strength of coarse waste materials using the B–K model was described and illustrated with data from seven waste materials from the banded iron formation in the Pilbara region of Western Australia. The definition of the input parameters of the model using the results of laboratory testing, field determinations and judgement was described, and the evaluation of the shear strength represented by the friction angle was carried out using deterministic and probabilistic approaches. The deterministic approach is based on using conservative values (25th percentile) of the input parameters, whereas the probabilistic approach uses probability distributions to represent them and a MC analysis to define the distribution of φ . In both cases, the objective was to account for the uncertainty in the properties of the waste material. The comparison of the deterministic results with the 75% confidence values from the probabilistic analysis indicates that the former are in general more conservative. This is because the probabilistic analysis takes into account the structure of the datasets and considers the propagation of the uncertainty of the parameters through the calculation process. The results of the probabilistic analysis presented in the paper correspond to the 75% confidence values, however, the level of confidence for a particular application needs to be selected so that it is consistent with the criterion of acceptability for the slope stability analysis. The use of the probabilistic results for design was examined and the selection of the appropriate values of friction angle for design considering spatial variability aspects of waste dumps was discussed.

Acknowledgement

The authors acknowledge the support of SRK Consulting and Fortescue Metals Group for preparing and presenting this paper.

References

- Barton, N 1973, 'Review of a new shear-strength criterion for rock joints', *Engineering Geology*, vol. 7, no. 4, pp. 287–332.
- Barton, N & Kjærnsli, B 1981, 'Shear strength of rockfill', *Journal of the Geotechnical Engineering Division*, vol. 107, no. GT7, pp. 873–891.
- Hawley, M & Cunning, J 2017, *Guidelines for Mine Waste Dump and Stockpile Design*, CSIRO Publishing, Clayton.
- Hungr, O, Dawson, R, Kent, A, Campbell, D & Morgenstern NR 2002, 'Rapid flow slides of coal mine waste in British Columbia, Canada', in *Catastrophic Landslides*, (Ed. SG Evans), Geological Society of America, Boulder, CO, pp. 191–208.
- Leps, TM 1970, 'Review of shearing strength of rockfill', *Journal of the Soil Mechanics and Foundations Division*, vol. 96, no. 4, pp. 1159–1170.
- Linero, S, Contreras, LF & Dixon, J 2022, 'Bayesian approach to improve the confidence of the estimation of the shear strength of very coarse mine waste using Barton's empirical criterion', *Proceedings of ICSMGE 2022: 20th International Conference on Soil Mechanics and Geotechnical Engineering*, Australian Geomechanics Society, St Ives, submitted for publication.
- Ovalle, C, Linero, S, Dano, C, Bard, E, Hicher, PY & Osses, R 2020, 'Data compilation from large drained compression triaxial tests on coarse crushable rockfill materials', *Journal of Geotechnical and Geoenvironmental Engineering*, vol. 146, no. 9.
- Renani, HR, Martin, CD, Varona, P & Lorig, L 2019, 'Stability analysis of slopes with spatially variable strength properties', *Rock Mechanics and Rock Engineering*, vol. 52, no. 10, pp. 3791–3808.